

***Ab initio* calculation of the elastic properties of $\text{Al}_{1-x}\text{Li}_x$ ($x \leq 0.20$) random alloys**A. Taga,¹ L. Vitos,^{1,2,3} B. Johansson,^{1,2} and G. Grimvall⁴¹*Applied Materials Physics, Department of Materials Science and Engineering, Royal Institute of Technology, SE-100 44 Stockholm, Sweden*²*Condensed Matter Theory Group, Physics Department, Uppsala University, SE-75121 Uppsala, Sweden*³*Research Institute for Solid State Physics and Optics, H-1525 Budapest, P.O. Box 49, Hungary*⁴*Theory of Materials, Physics Department, Royal Institute of Technology, Stockholm Center for Physics, Astronomy and Biotechnology, SE-106 91, Stockholm, Sweden*

(Received 26 April 2004; revised manuscript received 7 September 2004; published 5 January 2005)

Ab initio total energy calculations, based on the exact muffin-tin orbital (EMTO) theory, are used to determine the elastic properties of $\text{Al}_{1-x}\text{Li}_x$ random alloys ($x \leq 0.20$) in the face-centered-cubic crystallographic phase. The compositional disorder is treated within the framework of the single-site coherent potential approximation (CPA). The effect of the local lattice relaxation on the elastic constants is estimated using a supercell technique. We study the effect of the single-site approximation by comparing the theoretical ground-state properties calculated using different corrections to the Madelung energy. We find that the calculated equilibrium volumes and alloy formation energies strongly depend on the approximations employed in the Poisson equation, in accordance with former observations. At the same time, the experimental trends of the elastic moduli of disordered Al-Li alloys are well reproduced by the EMTO-CPA method. Using these theoretical results we show that the nonlinear effect of Li addition on the elastic constants originates from the detailed band structure of Al near the Fermi level.

DOI: 10.1103/PhysRevB.71.014201

PACS number(s): 71.15.Nc, 71.20.Gj, 62.20.Dc, 61.66.Dk

I. INTRODUCTION

During the 1980s and early 1990s Al-Li alloys were the focus of theoretical and experimental investigations.^{1–8} Other competing light-metal engineering materials have now emerged, but the complex electronic structure of Al-Li alloys^{6–9} and the observed interesting trends, such as the contraction of the equilibrium volume relative to a linear interpolation between Al Li (Ref. 10) and the drastic increase of the Young's and shear moduli on alloying Al Li (Ref. 11) have continued to be a scientific challenge.

Several successful theoretical efforts^{5–8} have concentrated on understanding the origin of this rather unusual behavior. Alloy theories based on the virtual crystal approximation¹² (VCA), coherent potential approximation^{13,14} (CPA), and cluster expansion approach^{15,16} have been used in the *ab initio* description of the ground-state properties of Al-Li. Although they reproduced the most characteristic features of the composition-dependent equilibrium volume, the theoretical mapping of the elastic properties against concentration has remained a problem. For instance, the pseudopotential-VCA method used by Vaks and Zein⁵ gave an incorrect elastic anisotropy and led to a sharp decrease of the Young's modulus above 5% Li, in contrast to the experiment.² The more advanced CPA-based calculation by Korzhavyi *et al.*⁷ was carried out within the atomic sphere approximation,¹⁷ which did not allow one to determine the single-crystal elastic constants.

An important aspect of modern *ab initio* electronic structure calculations in solids is that they can be used to establish high-resolution maps of physical properties in terms of crystal structure or chemical composition. Recent progress in the theory and methodology of disordered alloys^{18,19} has made it possible to extend the accurate quantum mechanical

calculations of elastic constants from ordered structures^{20,21} to the case of substitutional random alloys of any concentration.^{22–26} In the present work, using these developments, we give a detailed account of the elastic properties of face-centered-cubic (fcc) Al-Li binary solid solutions containing up to 20% randomly distributed Li. Our *ab initio* electronic structure study is based on the density functional theory²⁷ (DFT). The Kohn-Sham equations²⁸ are solved using the exact muffin-tin orbital (EMTO) method,^{9,19,29–32} and for the total energy calculation we employ the full charge density technique.^{19,33}

The substitutional disorder of Li atoms is taken into account using the coherent potential approximation implemented on the EMTO basis.¹⁸ Since in the CPA the impurity problem is treated within the single-site approximation, no information is obtained regarding the charge distribution around the solute atoms. During the last decade this deficiency of the CPA was analyzed by several research groups.^{7,34–42} It has been shown^{7,8,40} that an additional Madelung energy contribution, accounting for the charge transfer between alloy components, gives quantitatively improved properties compared to those obtained within the original single-site CPA. Here we study the role of this term in the case of the EMTO-CPA method. We show that the calculated equilibrium volumes and alloy formation energies crucially depend on the Madelung energy, in good agreement with former observations.^{7,8} However, we find that the elastic constants of Al-Li alloys are less sensitive to the single-site approximation and the EMTO-CPA method combined with an approximate Madelung term reproduces the observed trends in the elastic properties with an accuracy comparable to that of the DFT calculations for ordered structures.

Theoretical investigations of random alloys based on *ab initio* CPA-related methods usually neglect the local lattice

relaxation (LLR) around the impurity atoms. In some systems—e.g., Cu-Au alloys—the energy associated with LLR is comparable with the ordering energies, and therefore for these alloys the proper treatment of the lattice relaxations is an indispensable step.⁴³ In the present work, using a supercell technique, we study the LLR, and establish the order of magnitude of the effect of LLR on the elastic moduli of Al-Li solid solutions.

The rest of the paper is divided into two main sections and Conclusions. Section II presents the theoretical tools. This includes (a) an overview of the *ab initio* electronic structure calculation method, with special emphases on the technical details related to the single-site CPA, (b) a brief description of the single-crystal and polycrystal elastic moduli, and (c) the most important details of the numerical simulations. The results are presented and discussed in Sec. III.

II. THEORY

A. *Ab initio* EMTO-CPA method

The EMTO theory^{29–32} is an improved screened Korringa-Kohn-Rostoker method, where the exact one-electron potential $v(\mathbf{r})$ is represented by large overlapping muffin-tin potential spheres. By using overlapping spheres one describes more accurately the exact crystal potential, when compared to the conventional muffin-tin or nonoverlapping approach.^{19,30} The EMTO's are defined for each lattice site and for each angular momentum quantum number $L \equiv (l, m)$ with $l \leq l_{\max}$. They are constructed from the screened spherical waves, which are solutions of the wave equation with boundary conditions given in conjunction with nonoverlapping hard spheres.²⁹ Inside the potential spheres the low- l ($l \leq l_{\max}$) projections of the orbitals onto the spherical harmonics $Y_L(\hat{r})$ are the partial waves.²⁹ The matching between the screened spherical waves and the partial waves is realized at the hard spheres.²⁹

The Kohn-Sham equations²⁸ are solved for the optimized overlapping muffin-tin potential^{19,30,44} using the Green function formalism. In the case of random alloys the substitutional disorder is treated within the CPA.^{13,14} The average alloy density of states is determined from the average Green function, which, in turn, is obtained as the self-consistent solution of the CPA equations.^{18,44} The complete nonspherically symmetric charge density of the alloy component i is represented in one-center form around the lattice sites—i.e.,

$$n^i(\mathbf{r}) = \sum_L n_L^i(r) Y_L(\hat{r}), \quad (1)$$

where the sum includes the high- l (i.e., $l > l_{\max}$) partial density components $n_L^i(r)$ as well.^{19,44} In practice the high- l terms are truncated at $l_{\max}^h = 8-12$. The optimized overlapping muffin-tin potential is calculated from the full charge density $n^i(\mathbf{r})$, as described in Refs. 19 and 44.

Since the impurity problem in both the Schrödinger and Poisson equations is treated within the single-site approximation, the Coulomb system of a particular alloy component may contain a nonzero net charge. The effect of the charge

misfit on the potential is taken into account using the screened impurity model^{8,35,36,39} (SIM). According to this model the additional shift

$$\Delta v^{\text{SIM},i} = -\frac{2\alpha}{w} \left(Q^{i,s} - \sum_i c^i Q^{i,s} \right) \quad (2)$$

is added to the spherical part of the one-electron potential. Here $Q^{i,s}$ is the number of electrons inside the potential sphere, c_i the concentration of the alloy component i , and w the average atomic radius. The coefficient α in Eq. (2) controls the radius, where the net charge is redistributed around the impurity. With $\Delta v^{\text{SIM},i}$ expressed in atomic units, the suggested optimal value for the SIM parameter α is between ~ 0.6 and ~ 1.0 (Refs. 7, 8, 35, and 36).

Finally, within the EMTO method the total energy is calculated using the full charge density and the shape function techniques.^{33,44} In the case of random alloys the electrostatic energy includes the SIM correction term,^{8,35,36,39} which has the form

$$E^{\text{SIM}} = -\sum_i c^i \frac{\alpha'}{w} \left(Q^i - \sum_i c^i Q^i \right)^2, \quad (3)$$

where Q^i denotes the total number of electrons inside the Wigner-Seitz cell around the alloy component i . Most recent models of screening in the random alloys^{35,43} suggest a difference of $\sim 10\%$ between the coefficients α and α' from Eqs. (2) and (3). By using α' larger than α one can incorporate additional effects in E^{SIM} compared to $\Delta v^{\text{SIM},i}$, such as the multipole-multipole electrostatic interactions near the impurity. In the present application we neglect these effects and use $\alpha' = \alpha$.

The accuracy of the EMTO-CPA method has been demonstrated for the ground-state properties of metals, semiconductors, and oxides^{45–48} and binary ordered⁹ and random^{18,22–26} alloys.

B. Elastic properties

The elastic properties of crystals are given by the elements c_{ij} of the elasticity tensor. For a cubic lattice there are three independent elastic constants c_{11} , c_{12} , and c_{44} . The elastic anisotropy can be described, e.g., by the Every anisotropy parameter⁴⁹ $A_E = (c_{11} - c_{12} - 2c_{44}) / (c_{11} + c_{44})$. For an isotropic crystal we have $A_E = 0$. From the three elastic constants one obtains the longitudinal and transversal sound velocities. The average of them over all directions gives the sound velocity ν_D , which is used in the conventional Debye model with the Debye temperature defined as⁵⁰

$$\theta_D = (6\pi^2/V)^{1/3} (\hbar/k_B) \nu_D. \quad (4)$$

Here V is the atomic volume and \hbar and k_B are Planck's and Boltzmann's constants.

The main difference between the single-crystal alloys considered in first-principles calculations and the isotropic polycrystalline material is the inherent disorder in the grain orientations. The only way to establish first-principles parameters of these polycrystalline systems is to derive single-crystal values first and then to transform them to macro-

scopic quantities by suitable averaging methods. Here we adopt Hershey's averaging method,⁵¹ which has turned out to give the most accurate relation between single-crystal and polycrystalline data.⁵² Then, the average shear modulus G is given by the solution of the cubic equation

$$G^3 + \alpha G^2 + \beta G + \gamma = 0, \quad (5)$$

where

$$\alpha = (5c_{11} + 4c_{12})/8,$$

$$\beta = -c_{44}(7c_{11} - 4c_{12})/8,$$

$$\gamma = -c_{44}(c_{11} - c_{12})(c_{11} + 2c_{12})/8.$$

For a cubic lattice the average bulk modulus is identical to the single-crystal bulk modulus—i.e., $B = (c_{11} + 2c_{12})/3$. The Young's modulus is obtained from B and G as $E = 3BG/(3B + G)$.

C. Details of the numerical calculations

At each concentration the theoretical equilibrium volume V and the bulk modulus B were determined from a Murnaghan type function⁵³ fitted to the *ab initio* total energies of fcc structures for five different atomic volumes. In order to calculate the two cubic shear moduli $c' \equiv (c_{11} - c_{12})/2$ and c_{44} , we used the volume-conserving orthorhombic,

$$\begin{pmatrix} 1 + \varepsilon_o & 0 & 0 \\ 0 & 1 - \varepsilon_o & 0 \\ 0 & 0 & \frac{1}{1 - \varepsilon_o^2} \end{pmatrix}, \quad (6)$$

and monoclinic,

$$\begin{pmatrix} 1 & \varepsilon_m & 0 \\ \varepsilon_m & 1 & 0 \\ 0 & 0 & \frac{1}{1 - \varepsilon_m^2} \end{pmatrix}, \quad (7)$$

deformations, respectively. We calculated the total energies $E(\varepsilon_o) = E(0) + 2Vc'\varepsilon_o^2 + O(\varepsilon_o^4)$ and $E(\varepsilon_m) = E(0) + 2Vc_{44}\varepsilon_m^2 + O(\varepsilon_m^4)$ for six distortions $\varepsilon = 0.00, 0.01, \dots, 0.05$.

In the present application of the EMTO-CPA method to the Al-Li binary system the one-electron equations were solved within the scalar-relativistic and frozen-core approximations. The Green function was calculated for 16 complex energy points distributed exponentially on a semicircular contour. To obtain the accuracy needed for the calculation of elastic constants, we used about 15 000 uniformly distributed k points in the irreducible wedge of the orthorhombic and monoclinic Brillouin zones. However, at small concentrations a significantly higher number of k points ($\sim 10^5$) was needed for an accurate mapping of the reciprocal space. In the EMTO basis set we included s , p , and d orbitals ($l_{max} = 2$), and in the one-center expansion of the full charge density we used $l_{max}^h = 10$. The conventional Madelung energy⁴⁴ was calculated for $l_{max}^m = 8$. The self-consistent calculation

TABLE I. Theoretical (EMTO-CPA) and experimental (Expt.) equilibrium atomic volume V (in \AA^3), and bulk modulus B (in GPa) for Li and Al. Theoretical values were obtained for the fcc lattice using LDA, GGA, and LAG approximations for the exchange-correlation functional. Experimental data are listed for low-temperature hex(9) Li (Ref. 56) and for fcc Al (Ref. 11 and 56).

		LDA	GGA	LAG	Expt.
Li	V	18.98	20.02	20.43	21.06 ^a
	B	14.96	14.00	13.26	12.6 ^a
Al	V	15.95	16.54	16.38	16.61 ^a
	B	85.47	76.80	78.34	72.8, ^a 76.5 ^b

^aReference 56.

^bReference 11.

was performed within the local density approximation⁵⁴ (LDA) for the exchange-correlation functional, and, in addition to the LDA, the total energy was calculated using the generalized gradient approximation⁵⁵ (GGA) and the recently developed local Airy gas approximation⁴⁵ (LAG). For the SIM parameter we used two representative values $\alpha = 0.6$ and $\alpha = 0.9$. Finally, the radii of the overlapping muffin-tin spheres of Al and Li were chosen to be equal to the average atomic sphere radius w .

The effect of local lattice relaxation was studied using a supercell containing one Li and 15 Al atoms. First we calculated the equilibrium volume of the $\text{Al}_{15}\text{Li}_1$ system using a fixed fcc underlying lattice, and next we relaxed the first 12 nearest-neighbor Al atoms around the Li impurity. The tetragonal shear modulus c' was calculated for both fixed and relaxed supercell geometries, using ~ 2500 uniformly distributed k points in the irreducible wedge of the Brillouin zone. In the case of the orthorhombic distortion (6) the 12 nearest-neighbor Al atoms around a Li impurity are grouped in three different coordination shells, each of them consisting of 4 Al atoms. We performed additional relaxation for these 4-site shells for $\varepsilon_o = 0.05$ and found that the effect of relaxation on the total energy was comparable with the accuracy of our method. Therefore, in the elastic constant calculation we used the relaxed supercell geometry obtained for the undistorted lattice—i.e., for $\varepsilon_o = 0.00$.

III. RESULTS AND DISCUSSION

We evaluate the relative merits of the LDA, GGA, and LAG approximations to density functional theory in the case of Al-rich Al-Li alloys by comparing their performances for the equilibrium volume and elastic properties of pure metals. First we compare the present theoretical volume and bulk modulus of Li and Al, displayed in Table I, with the available experimental values. At low temperature and pressure Li has a close-packed, samarium-type hexagonal structure.⁵⁶ Here we approximate this structure by the fcc Li phase, which, however, is expected to have a minor effect on the equilibrium volume and bulk modulus. The difference between theoretical and experimental data from Table I is typical for what has been obtained for simple and transition metals^{45,57} in conjunction with the above approximations for the

TABLE II. Theoretical and experimental elastic constants (in GPa) and elastic anisotropy for fcc Al. The present theoretical values were obtained within LDA, GGA, and LAG approximations for the exchange-correlation functionals. References are given for the full-potential (FP) and experimental (Expt.) data.

	LDA	GGA	LAG	FP	Expt.
c_{11}	110.8	98.9	101.3	121.9 \pm 1.6, ^a 101.5 ^b 110.5, ^c 103.3 ^d	108, ^e 106.9 ^f 114.3 ^g
c_{12}	72.8	65.7	66.9	62.7 \pm 1.3, ^a 70.4 ^b 58.0, ^c 53.3 ^d	61, ^e 60.8 ^f 61.9 ^g
c_{44}	45.1	38.1	39.6	38.4 \pm 3.0, ^a 31.7 ^b 31.1, ^c 28.5 ^d	29, ^e 28.2 ^f 31.6 ^g
A_E	-0.79	-0.71	-0.73	-0.21, ^a -0.46 ^b -0.12, ^c -0.09 ^d	-0.13 ^{e,f,g}

^aReference 3, LAPW, LDA.

^bReference 60, LMTO, LDA.

^cReference 61, LMTO, GGA (Ref. 62).

^dReference 59, LAPW, LDA calculated at the experimental volumes.

^eReference 11.

^fReference 58.

^gExperimental values extrapolated to $T=0$ K, (Ref. 61).

exchange-correlation energy functional. The LDA strongly underestimates the equilibrium volumes and overestimates the bulk modulus for both metals. The GGA corrects this overbinding and reduces the mean LDA errors in V and B from -7% and 16% to -3% and 6% , respectively. We find that, on average, the LAG approximation outperforms both the LDA and GGA, giving errors -2% in volume and 5% in bulk modulus. However, when only Al is taken into account, the accuracy of the GGA is superior compared to that of the LAG approximation.

In Table II we list the calculated single-crystal elastic constants for fcc Al and compare them with the experimental data^{11,58} and former *ab initio* results calculated using full-potential (FP) linear augmented plane-wave^{3,59} (LAPW) and linear muffin-tin orbitals^{60,61} (LMTO) methods. We verify the accuracy of the EMTO-CPA method for anisotropic lattice distortions involved in elastic constant calculations by comparing our data with the FP values. If we let the error connected with such calculations be described by the difference between the FP results from Table II, the agreement between the present and former theoretical results is very good. Therefore, we have confidence in our data from Table II and use them to judge the performances of the LDA, GGA, and LAG for the elastic constants of fcc Al. The calculated average deviations between the experimental¹¹ and present theoretical data for cubic elastic constants, obtained within the LDA, GGA, and LAG, are 25% , 10% , and 13% , respectively. Thus, summing up the results from Tables I and II, we find that the GGA yields significantly better ground-state properties for Al compared to the LDA and marginally better compared to the LAG approximation. In the rest of the paper we will, therefore, present and discuss only results obtained within the GGA.

In Fig. 1 we present the calculated equilibrium volume and enthalpy of formation for Al-Li alloys as functions of concentration. Data are shown for two different α values

from Eqs. (2) and (3). We find that $\alpha \approx 0.9$ reproduces well the observed trend in the equilibrium volume, whereas $\alpha = 0.6$ gives an increase in V with Li addition, which is in between the experimental value and the one estimated from the linear rule of mixture. The enthalpy of formation of fcc $\text{Al}_{1-x}\text{Li}_x$ alloy is calculated as

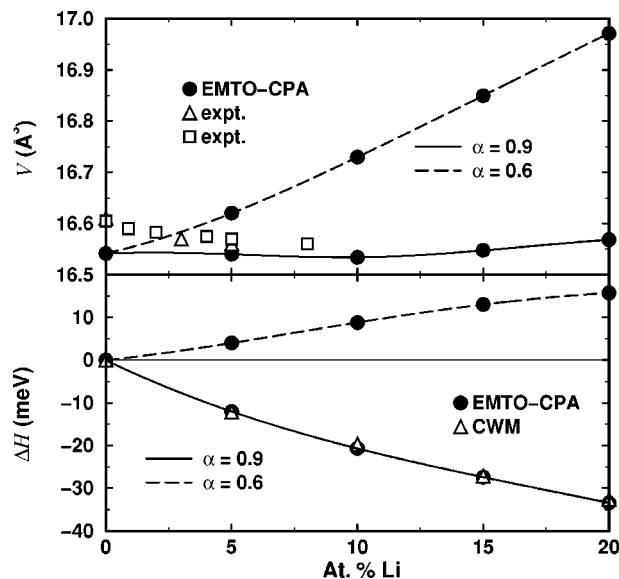


FIG. 1. Concentration dependence of the theoretical and experimental equilibrium atomic volume (upper panel) and mixing enthalpy (lower panel) of Al-Li random alloys. Experimental atomic volumes are from Ref. 10 (triangles) and Ref. 63 (squares). EMTO-CPA denotes the present results, and CWM stands for the results obtained using the Connolly-Williams method (Ref. 8). The two sets of EMTO-CPA results correspond to two different SIM parameters from Eqs. (2) and (3): $\alpha=0.9$ (solid line) and $\alpha=0.6$ (dashed line).

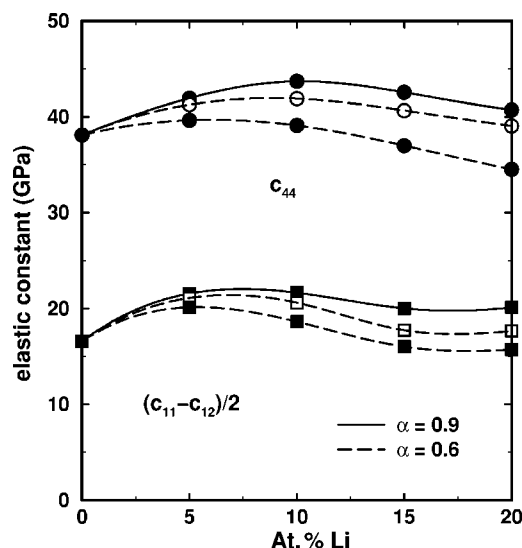


FIG. 2. Theoretical (EMTO-CPA) cubic shear moduli ($c_{11} - c_{12}$)/2 and c_{44} of Al-Li alloys as functions of Li content. Solid symbols correspond to the results obtained using $\alpha=0.9$ (solid line) and $\alpha=0.6$ (dashed line) in Eqs. (2) and (3). Open symbols denote results calculated at volumes corresponding to $\alpha=0.9$ and using $\alpha=0.6$ for the elastic constant calculations.

$$\Delta H(x) = E(\text{Al}_{1-x}\text{Li}_x) - (1-x)E(\text{Al}) - xE(\text{Li}),$$

where all the energies are obtained for the theoretical equilibrium volumes and expressed per atom. $E(\text{Al})$ and $E(\text{Li})$ are the total energies of fcc Al and Li, respectively. In Fig. 1 the present enthalpy of formation is compared with that obtained using the Connolly-Williams method⁸ (CWM). Within the CWM (Ref. 15) the Madelung energy is treated exactly and thus gives a good reference to establish the accuracy of our approach for the formation energy of completely random alloys. The perfect agreement in Fig. 1 between values calculated using the CWM and the present method with $\alpha=0.9$ demonstrates that the charge-transfer effects can be adequately taken into account in the single-site EMTO-CPA approach. Our result for $\Delta H(x)$ confirms the previous observations^{7,8} that the thermodynamic stability of Al-Li solid solutions is to a large extent determined by the Madelung energy accounting for the charge-transfer between Al and Li subsystems.

In Fig. 2 we illustrate the charge-transfer effects on the single-crystal elastic moduli of Al-Li alloys. The two sets of results for c' and c_{44} , marked by solid symbols connected with solid and dashed lines, were obtained from self-consistent EMTO-CPA calculations using $\alpha=0.9$ and $\alpha=0.6$, respectively. The variation of both sets of elastic constants with Li content is smooth. They exhibit similar concentration dependences, and the only important difference between them is the position of the maxima. We find that the maximum values in c' and c_{44} are shifted towards higher concentrations with increasing α . When the calculations are carried out at fixed volumes—e.g., those corresponding to $\alpha=0.9$ (shown by open symbols)—the effect of α is even less pronounced. The largest effect on the cubic shear moduli is obtained for $x=0.2$, where we get $\partial \ln c_{44} / \partial \ln \alpha \approx 0.45$.

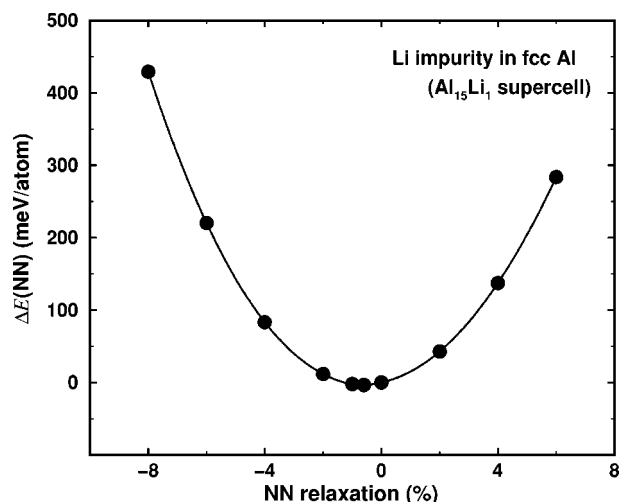


FIG. 3. Variation of the total energy of $\text{Al}_{15}\text{Li}_1$ supercell as a function of the nearest-neighbor (NN) Al-Li distance. The energy minimum corresponds to -0.6% inward relaxation of the first coordination shell around the Li impurity.

This variation is one order of magnitude smaller than $\partial \ln \Delta H(0.2) / \partial \ln \alpha \approx 4.42$, calculated for the enthalpy of formation (Fig. 1).

Next we address the question of LLR in Al-Li solid solutions. The present theoretical equilibrium volume of $\text{Al}_{15}\text{Li}_1$ supercell is 16.52 \AA^3 . This value is very close to 16.54 \AA^3 calculated for $\text{Al}_{0.9375}\text{Li}_{0.0625}$ random alloy using the CPA with $\alpha=0.9$. Figure 3 shows the variation of the total energy of $\text{Al}_{15}\text{Li}_1$ (ΔE) as a function of the nearest-neighbor (NN) Al-Li distance. From the energy minimum we find approximately -0.6% NN relaxation; i.e., in $\text{Al}_{15}\text{Li}_1$ the Al-Li distance decreases by 0.6% compared to the equilibrium Al-Al bond length in pure Al. The NN relaxation decreases the total energy relative to the unrelaxed structure by $\Delta E_{\min} \approx -3.3 \text{ meV/atom}$. Compared to other alloys, this relaxation can be considered very small.⁴³ Recently it was proposed that the LLR is mainly governed by the change of the volume of the host material.⁴³ The difference between the theoretical equilibrium volumes of $\text{Al}_{15}\text{Li}_1$ and fcc Al is $\sim 0.2\%$, which explains the small relaxation effects obtained in Al-Li solid solution.

The enthalpy of formation for a 16-atom supercell with an ideal fcc underlying lattice is calculated to be -21.6 meV/atom . With relaxed NN distance this energy decreases to -24.9 meV/atom . These numbers considerably exceed the mixing enthalpy of the $\text{Al}_{0.9375}\text{Li}_{0.0625}$ random alloy (Fig. 1). Using the data from Fig. 1 we estimate that $\alpha \approx 1.05 - 1.10$ would reproduce the supercell result for the formation energy. However, for a more accurate calculation of α one needs significantly larger supercells, where both the ordering energy and the energy due to the overlapping screening densities around Li atoms are negligible.

The present theoretical tetragonal shear modulus c' of $\text{Al}_{15}\text{Li}_1$ supercell with fcc underlying crystal structure is 20.3 GPa . The agreement between this value and $c' = 21.2 \text{ GPa}$, obtained for $\text{Al}_{0.95}\text{Li}_{0.05}$ random alloy using $\alpha=0.9$ (Fig. 2), is satisfactory, especially if one takes into account the numerical difficulties associated with elastic con-

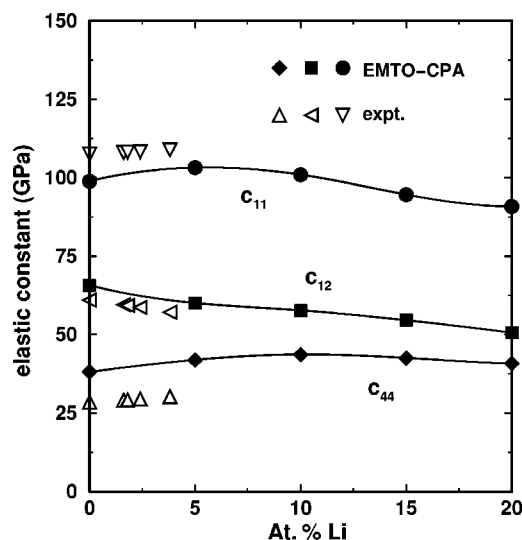


FIG. 4. Comparison between theoretical (present results) and experimental Ref. 11 single-crystal elastic constants for Al-Li random alloys.

stant calculations. A similar calculation carried out for a supercell with relaxed geometry corresponding to Fig. 3 gives $c' = 20.4$ GPa. Within the error bars of the present calculations this value is identical to that obtained for the unrelaxed geometry. The almost vanishing effect of the LLR on the elastic constant of Al-Li solid solutions can be ascribed to the small volume change on alloying. However, in systems where the lattice relaxation is more pronounced, like in Cu-Au alloys, a substantially larger impact of LLR on the elastic properties can be expected.

In Fig. 4 the present EMTO-CPA elastic constants for Al-Li random alloys, obtained using $\alpha = 0.9$ in Eqs. (2) and (3), are compared with the experimental data of Müller *et al.*¹¹ For all three elastic constants we find that the theoretical values and their variation with concentration are in good agreement with the experimental data. At Li contents below 5% the calculated changes with concentration in c_{11} , c_{12} , and c_{44} are 0.86, -1.13 , and 0.77 GPa per at. % Li, respectively. These numbers are close to the observed average variations 0.33, -0.95 , and 0.51 GPa per at. % Li (Ref. 11).

In the variation of the elastic constants c_{ij} with the concentration x of solute atoms in Fig. 4, we may single out that part which can be accounted for as due to an average change in the volume—i.e., in the lattice parameter. Data for higher-order elastic constants of Al give the pressure dependence $\partial c_{11}/\partial p = 5.9$, $\partial c_{12}/\partial p = 3.3$, and $\partial c_{44}/\partial p = 1.9$ (Ref. 50). From experiments⁶³ on the lattice parameter a of dilute Al-Li alloys we get $(1/a)(\partial a/\partial x) = -0.011$. When combined with the bulk modulus of Al, we get $\partial c_{11}/\partial x = 14.4$ GPa, $\partial c_{12}/\partial x = 8.1$ GPa, and $\partial c_{44}/\partial x = 4.6$ GPa. Thus, the effect of alloying on the lattice parameter would account for about half of the increase observed in c_{11} [~ 33 GPa (Ref. 11)], about 1/10 of the increase in c_{44} [~ 51 GPa (Ref. 11)], but it has a sign opposite to that observed for c_{12} (cf. Fig. 4). It follows that the Li solute atoms have an influence on c_{12} that depends crucially on the changes in the electronic structure. It is gratifying that our calculations correctly account for this differ-

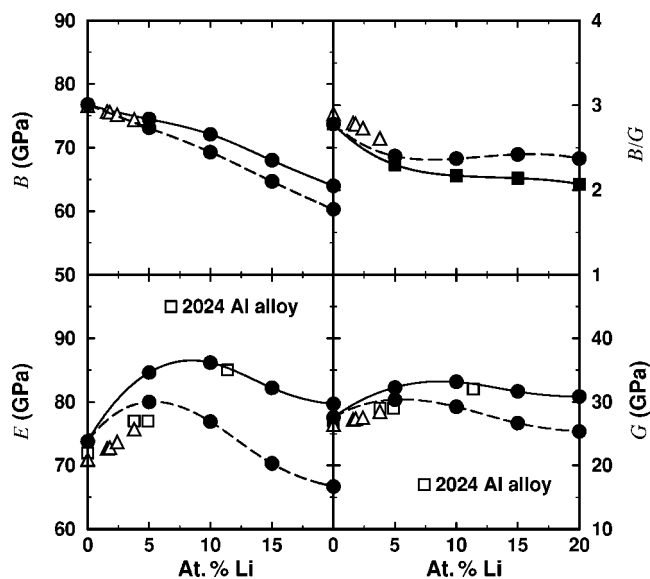


FIG. 5. Comparison between present theoretical (solid circles) and experimental (open triangles) (Ref. 11) polycrystalline elastic moduli (B , E , and G stand for bulk, Young's, and shear modulus, respectively) of Al-Li random alloys. Solid and dashed lines correspond to the two sets of self-consistent EMTO-CPA results from Fig. 2. For reference we also included experimental data for the Young's and shear moduli (open squares) obtained for the 2024 commercial aluminum alloy (Ref. 2).

ence between the trends of c_{12} and the other elastic constants.

The theoretical polycrystalline elastic moduli in Fig. 5 (solid lines) were calculated using single-crystal results from Fig. 4 and the averaging techniques presented in Sec. II B. In Fig. 5 we included the experimental data on Al-Li alloys by Müller *et al.*¹¹ and those on commercial 2024 aluminum alloy by Sankaran and Grant.² The observed decrease of the bulk modulus and the sharp increase of the Young's and shear moduli at low Li concentrations are well reproduced by the theory. In order to illustrate how sensitive the polycrystalline elastic moduli are to the value of α , in Fig. 5 the theoretical values obtained for $\alpha = 0.6$ are also shown (dashed lines). The small effect of α on the cubic elastic constants demonstrated in Fig. 2 can be evidenced also in the case of B and G . A somewhat larger effect is obtained for the Young's modulus, where the experimental value for 11.4% Li is poorly reproduced by the theoretical curve obtained for $\alpha = 0.6$. However, it is not clear whether the 18.3% Young's modulus enhancement in this commercial alloy, relative to that of pure Al, is due to the solid solution itself or to the intermetallic phase, which forms within the solid solution matrix above $\sim 12\%$ Li (Ref. 2).

The ratio between the bulk modulus and the shear modulus, shown in Fig. 5 as B/G , is a measure of the ductility of solids: ductile alloys are characterized by large B/G ratios, whereas low B/G ratios are representative of brittle solids.⁶⁴ We find that a small amount of Li makes the alloy more brittle compared to pure Al. In dilute Al-Li alloys the calculated B/G decreases with 9.6% per at. % Li, compared to the experimental decrease of 7.6%. We note that the opposite trend for c_{12} from Fig. 4, compared to c_{11} , leads to a rapid

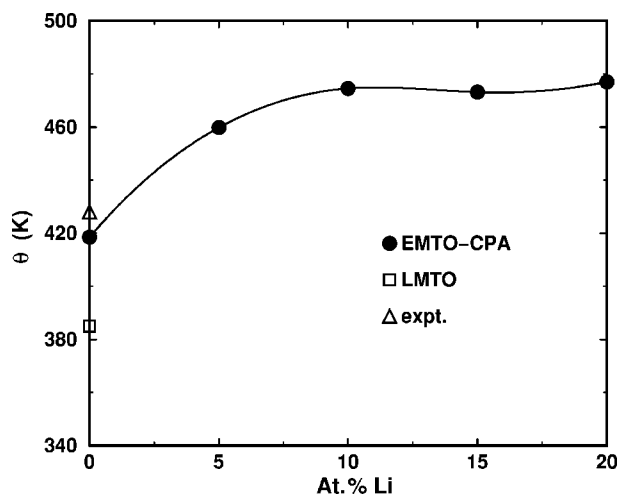


FIG. 6. Theoretical Debye temperatures of Al-Li alloys calculated using the EMTO-CPA method (present results) and the LMTO method (Ref. 60). The low-temperature experimental Debye temperature for Al is from Ref. 65.

increase in the cubic shear modulus $c' = (c_{11} - c_{12})/2$ and thus is essential for the observed rapid decrease in B/G on alloying Al with Li.

Finally, in Fig. 6 we present the low-temperature Debye temperatures as calculated from Eq. (4). The low-temperature experimental value for Al from Ref. 65 and the FP-LMTO value by Clouet *et al.*⁶⁰ are also included. According to our result, 10% Li addition to fcc Al increases the Debye temperature and, thus, the low-temperature limit of the heat capacity by 13%, in accordance with experiments.⁶⁶

We have demonstrated that the EMTO-CPA method with $\alpha \approx 0.9$ reproduces, with high accuracy, the observed trends of the elastic moduli of Al-Li random alloys. In the following we focus on the single-crystal elastic constants and investigate the peculiar concentration dependence of c' and c_{44} from Fig. 2. The two cubic shear moduli are proportional to the energy change $\Delta E(\varepsilon) = E(\varepsilon) - E(0)$ caused by a small lattice distortion ε relative to the high-symmetry structure. The electrostatic and exchange-correlation parts of $\Delta E(\varepsilon)$ are determined by the charge density $n^i(\mathbf{r})$. Our EMTO-CPA results show that the charge transfers and the multipole moments of $n^i(\mathbf{r})$ vary monotonously with Li concentration. Therefore we can exclude the electrostatic⁶⁷ or exchange-correlation origin of the observed unusual trend in the elastic constants.

In order to estimate the band energy part of $\Delta E(\varepsilon)$ and, thus, of the cubic shear moduli, first we analyze the density of states (DOS) of fcc Al-Li alloys. In Fig. 7 we compare the DOS of Al and of $\text{Al}_{0.9}\text{Li}_{0.1}$ and $\text{Al}_{0.8}\text{Li}_{0.2}$ alloys. The density of states of pure Al shows pronounced deviations from the free-electron-type behavior. The van Hove singularities near -4.5 , -2.7 , and -1.0 eV arise from the critical points in the band structure at L , X , and W symmetry points from the Brillouin zone.⁶⁸ The Fermi level (E_F) of Al is situated above the W minimum. Thus we expect that a small amount of Li addition—i.e., a small decrease in the number of electrons—would shift the position of E_F towards the W singularity. Indeed, we find that at 10% Li the Fermi level is located at the W minimum, and with increasing Li concentration E_F is

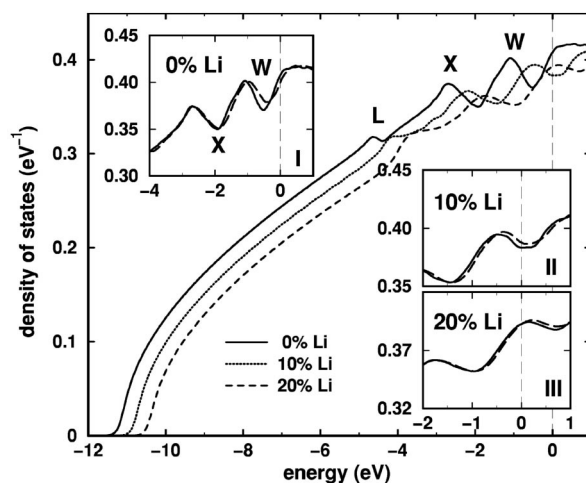


FIG. 7. Calculated density of state of fcc Al-Li alloys encompassing 0 (solid line), 10 (dotted line) and 20 (dashed line) at. % Li. In the insets the fcc densities of states (solid lines), shown on enlarged scales, are compared to the densities of states of a monoclinic structure (dashed lines) corresponding to the monoclinic deformation (7) with $\varepsilon_m = 0.05$. Vertical dashed lines denote the position of the Fermi level.

moved towards the W maximum. Note that in spite of the smearing effect of the disordered substitutional Li, at 20% Li we still can identify the main DOS structures characteristic of pure Al.

We illustrate the effect of lattice distortion on the DOS of Al-Li alloys by considering the monoclinic distortion (7) with $\varepsilon_m = 0.05$. In insets I–III in Fig. 7 we compare the DOS of fcc alloys with the DOS calculated for alloys having the monoclinic structure. We find that the symmetry-lowering monoclinic distortion leaves the X singularity almost unchanged, whereas it slightly alters and shifts the position of the W minimum to higher energies. As a result, we obtain that the density of states at the Fermi level decreases with monoclinic distortion in pure Al, increases in $\text{Al}_{0.9}\text{Li}_{0.1}$, and remains constant in $\text{Al}_{0.8}\text{Li}_{0.2}$. Therefore, the band energy contribution to $\Delta E(\varepsilon_m)$ is negative in the case of Al, positive for intermediate (approximately 5%–15%) Li concentrations, and zero for $\sim 20\%$ Li. This results in a maximum in c_{44} near 10 at. % Li (Fig. 2). A similar mechanism is responsible for the concentration dependence of the tetragonal shear modulus c' .

IV. CONCLUSIONS

Using the EMTO-CPA *ab initio* total energy method we have calculated the elastic properties of random Al-Li binary alloys. Where comparison is possible good agreement is found with the experimental data for both single-crystal and polycrystalline elastic moduli. The most surprising result of the present work is the small effect of the Madelung correction term on the calculated elastic properties, compared to the one observed in the case of the enthalpy of formation. This is a consequence of the error cancellation between the total energies of slightly different structures involved in the calculation of the elastic constants. Our results imply that the

screening around the impurities in metallic systems depends on the type of the atoms [described by the net charge from Eqs. (2) and (3)] and the average atomic radius, but shows weak structural dependence. Using the EMTO-CPA method, in combination with the SIM for the electrostatic contributions, we have investigated the origin of the peculiar concentration dependence of the elastic constants of Al-Li random alloys. We have found that the observed nonlinear effect of Li addition on the elastic constants results from the particular band structure of Al near the Fermi level.

Since the Al-Li system presents one of the most severe tests for single-site CPA-based methods, the present finding suggests that the EMTO-CPA method can safely be applied to the *ab initio* determination of the elastic properties of substitutional random alloys. The obtained overall good

agreement with experiment demonstrates the applicability of the present quantum mechanical method for mapping the elastic properties of random alloys against chemical composition.

ACKNOWLEDGMENTS

This work was supported by the Swedish Research Council, the Swedish Foundation for Strategic Research, the Royal Swedish Academy of Sciences, and research Project Nos. OTKA T035043 and T046773 of the Hungarian Scientific Research Fund. The calculations were performed at the Swedish National Supercomputer Center, Linköping and Hungarian National Supercomputer Center, Budapest.

-
- ¹See, e.g., *Aluminium-Lithium Alloys*, edited by C. Baker *et al.* (London Institute of Metals, London, 1986), Vol. III.
- ²K. K. Sankaran and N. J. Grant, *Mater. Sci. Eng.* **44**, 213 (1980).
- ³M. J. Mehl, *Phys. Rev. B* **47**, 2493 (1993).
- ⁴M. H. F. Sluiter, Y. Watanabe, D. de Fontaine, and Y. Kawazoe, *Phys. Rev. B* **53**, 6137 (1996).
- ⁵V. G. Vaks and N. E. Zein, *J. Phys.: Condens. Matter* **2**, 5919 (1990).
- ⁶M. Sluiter, D. de Fontaine, X. Q. Guo, R. Podloucky, and A. J. Freeman, *Phys. Rev. B* **42**, 10 460 (1990).
- ⁷P. A. Korzhavyi, A. V. Ruban, S. I. Simak, and Yu. Kh. Vekilov, *Phys. Rev. B* **49**, 14 229 (1994).
- ⁸P. A. Korzhavyi, A. V. Ruban, I. A. Abrikosov, and H. L. Skriver, *Phys. Rev. B* **51**, 5773 (1995).
- ⁹L. Vitos, H. L. Skriver, B. Johansson, and J. Kollár, *Comput. Mater. Sci.* **18**, 24 (2000).
- ¹⁰S. H. Kellington, D. Loveridge, and J. M. Titman, *Br. J. Appl. Phys.*, *J. Phys. D* **2**, 1162 (1969).
- ¹¹W. Müller, E. Bubeck, and V. Gerold, in *Aluminium-Lithium Alloys*, edited by C. Baker *et al.* (London Institute of Metals, London, 1986), Vol. III, 435.
- ¹²P. J. Wojtowicz and J. G. Kirkwood, *J. Chem. Phys.* **33**, 1299 (1960).
- ¹³P. Soven, *Phys. Rev.* **156**, 809 (1967).
- ¹⁴B. L. Györfy, *Phys. Rev. B* **5**, 2382 (1972).
- ¹⁵J. W. D. Connolly and A. R. Williams, *Phys. Rev. B* **27**, 5169 (1983).
- ¹⁶J. M. Sanchez, F. Ducastelle, and D. Gratias, *Physica A* **128**, 334 (1984).
- ¹⁷H. L. Skriver, *The LMTO Method* (Springer-Verlag, Berlin, 1984).
- ¹⁸L. Vitos, I. A. Abrikosov, and B. Johansson, *Phys. Rev. Lett.* **87**, 156401 (2001).
- ¹⁹L. Vitos, *Phys. Rev. B* **64**, 014107 (2001).
- ²⁰J. M. Wills, O. Eriksson, P. Söderlind, and A. M. Boring, *Phys. Rev. Lett.* **68**, 2802 (1992).
- ²¹P. Söderlind, O. Eriksson, J. M. Wills, and A. M. Boring, *Phys. Rev. B* **48**, 5844 (1993).
- ²²L. Vitos, P. A. Korzhavyi, and B. Johansson, *Nat. Mater.* **2**, 25 (2003).
- ²³B. Magyari-Köpe, G. Grimvall, and L. Vitos *Phys. Rev. B* **66**, 064210 (2002).
- ²⁴B. Johansson, L. Vitos, and P. A. Korzhavyi, *Solid State Sci.* **5**, 931 (2003).
- ²⁵P. Olsson, I. A. Abrikosov, L. Vitos, and J. Wallenius *J. Nucl. Mater.* **321**, 84 (2003).
- ²⁶L. Vitos, P. A. Korzhavyi, and B. Johansson, *Phys. Rev. Lett.* **88**, 155501 (2002).
- ²⁷P. Hohenberg and W. Kohn, *Phys. Rev.* **136**, B864 (1964).
- ²⁸W. Kohn and L. J. Sham, *Phys. Rev.* **140**, 1133 (1965).
- ²⁹O. K. Andersen, O. Jepsen, and G. Krier, in *Lectures on Methods of Electronic Structure Calculations*, edited by V. Kumar, O. K. Andersen, and A. Mookerjee (World Scientific, Singapore, 1994), p. 63.
- ³⁰O. K. Andersen, C. Arcangeli, R. W. Tank, T. Saha-Dasgupta, G. Krier, O. Jepsen, and I. Dasgupta, in *Tight-Binding Approach to Computational Materials Sciences*, edited by P. E. A. Tunchi, A. Gonis, and L. Colombo, MRS Symposia Proceedings No. 491 (Materials Research Society, Pittsburgh, 1998), p. 3.
- ³¹O. K. Andersen, T. Saha-Dasgupta, R. W. Tank, C. Arcangeli, O. Jepsen, and G. Krier, in *Electronic Structure and Physical Properties of Solids: The uses of the LMTO method*, edited by H. Dreyssé, Lectures Notes in Physics (Springer-Verlag, Berlin, 2000), p. 3.
- ³²O. K. Andersen and T. Saha-Dasgupta, *Phys. Rev. B* **62**, R16 219 (2000).
- ³³J. Kollár, L. Vitos, and H. L. Skriver, in *Electronic Structure and Physical Properties of Solids: The Uses of the LMTO Method*, edited by H. Dreyssé, Lectures Notes in Physics (Springer-Verlag, Berlin, 2000), p. 85.
- ³⁴A. V. Ruban, I. A. Abrikosov, and H. L. Skriver, *Phys. Rev. B* **51**, 12 958 (1995).
- ³⁵A. V. Ruban and H. L. Skriver, *Phys. Rev. B* **66**, 024201 (2002).
- ³⁶A. V. Ruban, S. I. Simak, P. A. Korzhavyi, and H. L. Skriver, *Phys. Rev. B* **66**, 024202 (2002).
- ³⁷R. Magri, S.-H. Wei, and A. Zunger, *Phys. Rev. B* **42**, 11 388 (1990).
- ³⁸Z. W. Lu, S.-H. Wei, A. Zunger, S. Frota-Pessoa, and L. G. Ferreira, *Phys. Rev. B* **44**, 512 (1991).
- ³⁹D. D. Johnson and F. J. Pinski, *Phys. Rev. B* **48**, 11 553 (1993).

- ⁴⁰I. A. Abrikosov, Yu. H. Vekilov, P. A. Korzhavyi, A. V. Ruban, and L. E. Shilkrot, *Solid State Commun.* **83**, 867 (1992).
- ⁴¹P. P. Singh, A. Gonis, and P. E. A. Turchi, *Phys. Rev. Lett.* **71**, 1605 (1993).
- ⁴²P. P. Singh and A. Gonis, *Phys. Rev. B* **49**, 1642 (1994).
- ⁴³A. V. Ruban, S. I. Simak, S. Shallcross, and H. L. Skriver, *Phys. Rev. B* **67**, 214302 (2003).
- ⁴⁴L. Vitos, *Recent Research Developments in Physics* (Transworld Research Network Publisher, Trivandrum, India, 2004), Vol. 5, pp. 103–140.
- ⁴⁵L. Vitos, B. Johansson, J. Kollár, and H. L. Skriver, *Phys. Rev. B* **62**, 10 046 (2000).
- ⁴⁶L. Vitos, B. Johansson, and J. Kollár, *Phys. Rev. B* **62**, R11 957 (2000).
- ⁴⁷B. Magyari-Köpe, L. Vitos, and J. Kollár, *Phys. Rev. B* **63**, 104111 (2001).
- ⁴⁸B. Magyari-Köpe, L. Vitos, B. Johansson, and J. Kollár, *Acta Crystallogr., Sect. B: Struct. Sci.* **57**, 491 (2001).
- ⁴⁹A. G. Every, *Phys. Rev. B* **22**, 1746 (1980).
- ⁵⁰G. Grimvall, *Thermophysical Properties of Materials*, enlarged and revised ed. (North-Holland, Amsterdam, 1999).
- ⁵¹H. M. Ledbetter, *J. Appl. Phys.* **44**, 1451 (1973).
- ⁵²H. M. Ledbetter, in *Handbook of Elastic Properties of Solids, Liquids, Gases*, edited by M. Levy, H. E. Bass, and R. R. Stern (Academic, San Diego, 2001), Vol. III, pp. 313–324.
- ⁵³C.-L. Fu and K.-M. Ho *Phys. Rev. B* **28**, 5480 (1983).
- ⁵⁴J. P. Perdew and Y. Wang, *Phys. Rev. B* **45**, 13 244 (1992).
- ⁵⁵J. P. Perdew, K. Burke, and M. Ernzerhof, *Phys. Rev. Lett.* **77**, 3865 (1996).
- ⁵⁶D. A. Young, *Phase Diagrams of the Elements* (University of California Press, Berkeley, 1991).
- ⁵⁷S. Kurth, P. J. Perdew, and P. Blaha, *Int. J. Quantum Chem.* **75**, 889 (1999).
- ⁵⁸G. N. Kamm and G. A. Alers, *J. Appl. Phys.* **35**, 327 (1964).
- ⁵⁹S. H. Yang, M. J. Mehl, and D. A. Papaconstantopoulos, *Phys. Rev. B* **57**, R2013 (1998).
- ⁶⁰E. Clouet, J. M. Sanchez, and C. Sigli, *Phys. Rev. B* **65**, 094105 (2002).
- ⁶¹G. V. Sinko and N. A. Smirnov, *J. Phys.: Condens. Matter* **14**, 6989 (2002).
- ⁶²J. P. Perdew, J. A. Chevary, S. H. Vosko, K. A. Jackson, M. R. Pederson, D. J. Singh, and C. Fiolhais, *Phys. Rev. B* **46**, 6671 (1992).
- ⁶³H. J. Axon and W. Hume-Rothery, *Proc. R. Soc. London, Ser. A* **193**, 1 (1948).
- ⁶⁴S. F. Pugh, *Philos. Mag.* **45**, 823 (1954).
- ⁶⁵C. Kittel, *Introduction to Solid State Physics*, 7th ed. (Wiley, New York, 1996).
- ⁶⁶A. G. Fox and R. M. Fisher, *J. Mater. Sci. Lett.* **7**, 301 (1988).
- ⁶⁷V. L. Moruzzi, J. F. Janak, and A. R. Williams, in *Calculated Electronic Properties of Metals* (Pergamon, New York, 1978).
- ⁶⁸N. W. Ashcroft, *Phys. Rev. B* **19**, 4906 (1979).